JCB Article

c-erbB-3: a nuclear protein in mammary epithelial cells

Martin Offterdinger,[1] Christian Schöfer,[2] Klara Weipoltshammer,[2] and Thomas W. Grunt[1]

[1]Signaling Networks Program, Division of Oncology, Department of Internal Medicine I, University of Vienna, A-1097 Vienna, Austria
[2]Institute for Histology and Embryology, University of Vienna, A-1090 Vienna, Austria

C-erbB receptors are usually located in cell membranes and are activated by extracellular binding of EGF-like growth factors. Unexpectedly, using immunofluorescence we found high levels of c-erbB-3 within the nuclei of MTSV1-7 immortalized nonmalignant human mammary epithelial cells. Nuclear localization was mediated by the COOH terminus of c-erbB-3, and a nuclear localization signal was identified by site-directed mutagenesis and by transfer of the signal to chicken pyruvate kinase. A nuclear export inhibitor caused accumulation of c-erbB-3 in the nuclei of other mammary epithelial cell lines as demonstrated by immunofluorescence and biochemical cell fractionation, suggesting that c-erbB-3 shuttles between nuclear and nonnuclear compartments in these cells. Growth of MTSV1-7 on permeable filters induced epithelial polarity and concentration of c-erbB-3 within the nucleoli. However, the c-erbB-3 ligand heregulin β1 shifted c-erbB-3 from the nucleolus into the nucleoplasm and then into the cytoplasm. The subcellular localization of c-erbB-3 obviously depends on exogenous stimuli and on the stage of epithelial polarity and challenges the specific function of c-erbB-3 as a transmembrane receptor protein arguing for additional, as yet unidentified, roles of c-erbB-3 within the nucle(ol)us of mammary epithelial cells.

Introduction

c-erbB-1 to -4 are generally considered as transmembrane receptors, which usually exert their activities through extracellular binding of EGF-like growth factors. Ligand-stimulated c-erbB-1, -2, and -4 phosphorylate themselves and other cytoplasmic substrates at tyrosine residues, thus activating an intracellular signaling cascade. c-erbB-1 and -2 represent useful parameters for the prognosis of malignant diseases (Grunt and Huber, 1994) and are used as target structures for anticancer therapeutics (Shepard et al., 1991; Osherov et al., 1993). Heregulin (HRG)* binds to c-erbB-3 or -4 and induces heterodimerization of these receptors with c-erbB-2. The latter thus represents an orphan receptor that does not bind HRG on its own but reveals potent tyrosine kinase activity and acts as a coreceptor molecule that is crucial for HRG-dependent signaling. c-erbB-3, like the other c-erbB receptors, contains one predicted transmembrane domain (MALTVIAGLVVIFMMLGGTFL, amino acids 644–664), but in contrast to the other members it does not have a functional tyrosine kinase domain (Guy et al., 1994). Thus, c-erbB-3 requires a heterodimer partner for tyrosine kinase signaling. The COOH terminus of c-erbB-3, in turn, reveals potent signaling capability by direct recruitment of phosphatidylinositol 3-kinase and Shc (Waterman et al., 1999). All c-erbB receptors can form functionally active heterodimers (Riese et al., 1996). However, the described activities explain why the c-erbB-2/-3 dimer constitutes the most active c-erbB receptor complex (Pinkas-Kramarski et al., 1996). c-erbB-3, unlike c-erbB-2, is present in most human tissues (Prigent et al., 1992). In breast cancer cells, both can be overexpressed/activated separately or jointly, can cooperate during transformation and progression (Kraus et al., 1989, 1993; Lemoine et al., 1992; Rajkumar and Gullick, 1994; Alimandi et al., 1995), and can be found not only in the cell membrane but also in intracellular compartments (Kumar et al., 1991; Lemoine et al., 1992).

Nontumorigenic MTSV1-7 cells represent milk derived, SV40 large T antigen–immortalized, nonmalignant human mammary epithelial cells that express cytokeratins 7, 8, 18, and 19 and reveal a morphology, which is indicative of their luminal origin (Bartek et al., 1991).

Here we demonstrate nuclear localization of c-erbB-3 in MTSV1-7 and in human breast cancer cells, which is due to an active nuclear localization signal (NLS) near the COOH

Address correspondence to Thomas W. Grunt, Signaling Networks Program, Div. of Oncology, Dept. of Internal Medicine I, University of Vienna, Währinger Gürtel 18-20, A-1097 Vienna, Austria. Tel.: 43-1-40400-5487. Fax: 43-1-40400-5465. E-mail: thomas.grunt@akh-wien.ac.at

M. Offterdinger's present address is Cell Biology and Cell Biophysics Programme, European Molecular Biology Laboratory (EMBL)-Heidelberg, Meyerhofstr. 1, D-69117 Heidelberg, Germany.

*Abbreviations used in this paper: C, cytoplasmic-enriched; CRM, chromatin region maintenance; CPK, chicken pyruvate kinase; EGFP, enhanced green fluorescent protein; HRG, heregulin; LMB, leptomycin B; N, nuclear-enriched; NLS, nuclear localization signal; PFA, paraformaldehyde.

Key words: c-erbB-3; epithelial polarity; heregulin; mammary epithelial cells; nuclear localization

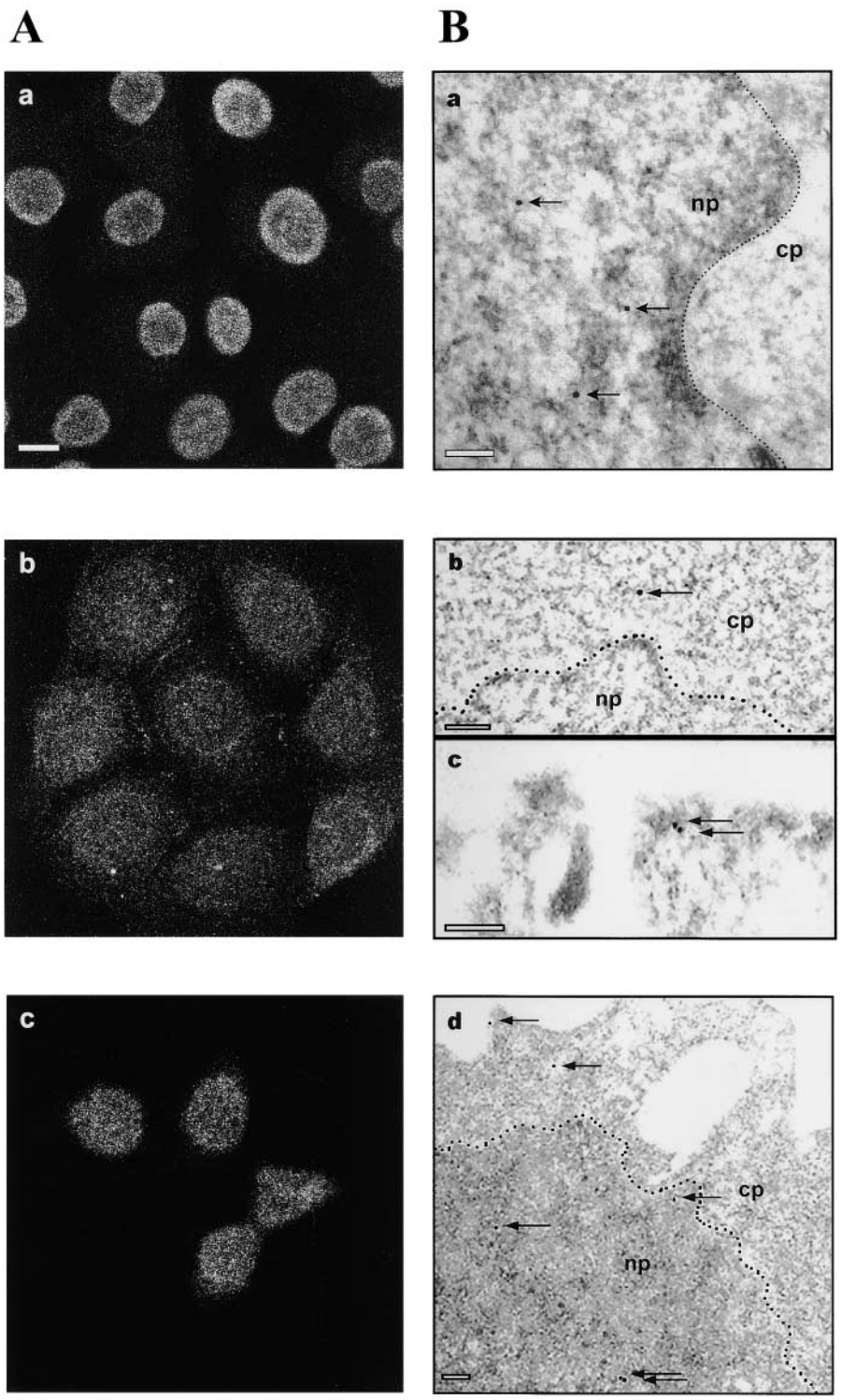

Figure 1. **Nuclear localization of c-erbB-3 in MTSV1-7.** (A) Confocal immunofluorescent microscopy demonstrating nuclear c-erbB-3 using the monoclonal RTJ2 antibody directed against a cytoplasmic epitope of c-erbB-3 (a) or polyclonal antibodies against an NH_2- (b, Ab-9) or COOH-terminal domain (c, C17). Note in panel b some cytoplasmic and membrane staining is also seen. Bar, 25 μm. (B) Immuno EM using RTJ2 (a–c) and Ab-9 (d) revealing nuclear (a and d), cytoplasmic (b and d), and cell membrane-located (c and d) c-erbB-3 (arrows). np, nucleoplasm; cp, cytoplasm. Bars, 0.1 μm.

terminus of the protein. Moreover, c-erbB-3 was found in the nucleoli of differentiated polarized MTSV1-7 and exported into the cytoplasm upon addition of exogenous HRG.

Results

Nuclear localization of c-erbB-3

Subcellular distribution of c-erbB-3 was examined in MTSV1-7 cells by confocal immunofluorescence microscopy and immuno EM. Fig. 1 A reveals nuclear immunofluorescence obtained with three different c-erbB-3–specific antibodies: a monoclonal antibody directed against a cytoplasmic epitope of c-erbB-3 (RTJ2) produced a strong nuclear signal (Fig. 1 A, a); staining of the nuclei was slightly less intense when polyclonal antibodies reacting either with a domain close to the extracellular NH_2 terminus (Ab-9) (Fig. 1 A, b) or with the cytoplasmic COOH terminus of c-erbB-3 (C17) (Fig. 1 A, c) were used. It has to be noted that Ab-9 also weakly labeled some cytoplasmic and membrane sites (Fig. 1 A, b). Equivalent staining was obtained with three different

Table I. **Quantification of label density distribution after immuno EM using c-erbB-3 specific antibodies**[a]

Antibody	Mean label density (SD)	
	Nucleus	**Cytoplasm**
RTJ2	55.06 (48.72)	3.60 (2.91)*
Ab-9	46.81 (37.12)	26.62 (16.93)**
Control	0.30 (0.96)	0.35 (0.63)

[a]Signal density after immunostaining with monoclonal RTJ2, polyclonal Ab-9, or without first antibody (control) was evaluated as gold grains per nuclear and cytoplasmic area of 10 randomly chosen cells per sample ([number of gold grains/μm^2] $\times$ 100). High values for SDs are due to variability of total cellular label densities amongst individual cells. The nuclear label density produced by RTJ2 consistently was between 82 and 95% of the total cellular label density, whereas for Ab-9 it ranged from 65 to 84%. Cytoplasmic label densities in the presence of RTJ2 and Ab-9 were significantly higher than in controls as evaluated with Student's *t* test. $*P < 0.01$; $**P < 0.001$.

protocols for cell fixation and permeabilization (unpublished data). The data suggest that nuclear c-erbB-3 is not truncated but rather represents the full-length protein and that the occurrence of c-erbB-3 in the nuclei is not an artifact caused by the cell preparation. This specific pattern of subcellular distribution of c-erbB-3 was further confirmed by immuno EM. Nuclear staining was obtained with the RTJ2 and Ab-9 antibodies (Figs. 1 B, a and d), respectively. Moreover, both antibodies also labeled some cytoplasmic (Figs. 1 B, b and d) and cell membrane sites (Figs. 1 B, c and d). Two other antibodies gave only very weak (C17) or no signals at all (SGP1) und thus were not suitable for EM (unpublished data).

A quantitative analysis of these data (Table I) demonstrates that both RTJ2 and Ab-9 preferentially stain the nuclei of MTSV1-7 cells, although at varying relative intensities. For RTJ2, the mean nuclear/nonnuclear distribution of the immunogold label was ~15:1, whereas for Ab-9 it was 1.8:1. The intensity of the total (nucleus plus cytoplasm) background signal was ~1% of the total stains obtained with RTJ2 and Ab-9, respectively, and with both antibodies label density in the cytoplasm was significantly higher than that in the cytoplasm of the negative controls (Table I).

We hypothesized that nuclear localization might be a general property of c-erbB-3. Therefore, a panel of nonmalignant and malignant human mammary epithelial cells was subjected to immunofluorescence microscopy in the absence or presence of the nuclear export inhibitor leptomycin B (LMB). This drug specifically blocks the chromatin region maintenance (CRM)1 nuclear export factor by covalent modification (Kudo et al., 1999). In MCF10A, MCF-7, T47D (Fig. 2 A), and BT474 cells (unpublished data), LMB clearly caused nuclear concentration of c-erbB-3. In BT20 and MDA468 cells, nuclear staining was strong already in the absence of LMB and was not further intensified by LMB (Fig. 2 A). Similar results were obtained in MTSV1-7 (unpublished data). BT483 revealed a very low growth rate (splitting ratio 1:2 per 2 wk) and was the only cell line that showed neither spontaneous nor LMB-induced nuclear c-erbB-3 staining. Instead, BT483 showed cytoplasmic and plasma membrane staining for c-erbB-3 (Fig. 2 A). Fig. 2 B demonstrates the subcellular distribution of transiently expressed FLAG-tagged c-erbB-3 in MCF-7 cells after immunolabeling with an anti-FLAG antibody. Vehicle-treated

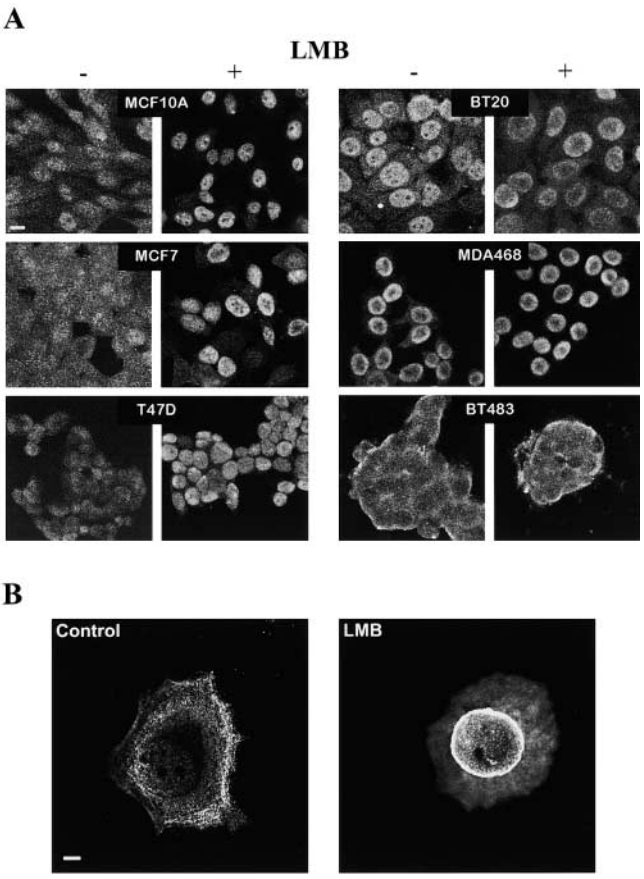

Figure 2. **Effects of LMB on the subcellular distribution of c-erbB-3 using confocal immunofluorescence microscopy.** (A) Various cell lines were treated for 24 h with solvent (−) or 20 ng/ml LMB (+) and immunostained using RTJ2. Bar, 25 μm. (B) MCF-7 cells were transiently transfected with FLAG-tagged c-erbB-3, treated for 24 h with solvent (Control) or 5 ng/ml LMB, and immunostained with M2 anti-FLAG antibody. Bar, 5 μm.

control cells revealed predominantly cytoplasmic staining, whereas LMB-exposed (5 ng/ml, 24 h) MCF-7cells displayed nuclear accumulation of c-erbB-3–FLAG. Interestingly, c-erbB-2, representing the most important heterodimer partner of c-erbB-3, did not localize to the nucleus of any of the cell lines tested neither spontaneously nor after LMB treatment and independent of the level of spontaneous expression (unpublished data).

Surprisingly, although c-erbB-3 is known as a transmembrane protein, c-erbB-3–specific immunofluorescent labeling at the surface membranes was barely visible in most cell lines studied. Outshining effects due to more prominent nuclear and cytoplasmic immunostaining might partially cause this. Therefore, nonpermeabilized cells were subjected to flow cytometry using the SGP1 monoclonal antibody, which recognizes an extracellular epitope of c-erbB-3. All cells were life gated with propidium iodide in order to exclude intercellular staining of nonviable cells.

Table II demonstrates that all cell lines analyzed except BT20 contained c-erbB-3 within the surface membrane, albeit at varying intensities.

Next, we wanted to confirm the nuclear expression of c-erbB-3 by using a nonmicroscopy-based system. To this end, proteins from MCF-7 cell lysates were subjected to sub-

Table II. **Cell surface expression of c-erbB-3 as demonstrated by flow cytometry**[a]

Cell line	MFI[b]	
	mIgG	c-erbB-3
MCF-7	2.09	17.20
MDA468	3.22	11.74
T47D	1.76	4.81
BT20	2.01	2.54

[a]A minimum of 5,000 nonpermeabilized cells was stained with murine IgG or with SGP1 anti–c-erbB-3 and anti–mouse Ig Alexa 488 conjugate. Life gating with propidium iodide was performed in order to exclude permeable cells from analysis.
[b]MFI, mean fluorescence intensity (arbitrary units).

cellular fractionation followed by immunoprecipitation and Western blotting. Cytoplasmic-enriched (C) and nuclear-enriched (N) protein fractions of untreated and LMB-treated (24 h, 5 ng/ml) MCF-7 cells were precipitated with a monoclonal antibody against the extracellular domain of c-erbB-3 (SGP1) followed by blotting with an affinity purified polyclonal antibody against an intracellular peptide of c-erbB-3 (C17). Fig. 3 A demonstrates that LMB induced a significant shift of c-erbB-3 from the C into the N fraction. Densitometric quantitation of the band intensities in C and N was done, and the relative distribution between the compartments was expressed as a C to N ratio, which dropped from 3.0 before LMB to <0.8 after LMB treatment. Equivalent results were obtained when c-erbB-3 was probed by Western blotting without immunoprecipitation (C17 only) (Fig. 3 B). The purity of the fractions was estimated by probing Western blot membranes for the following marker proteins (Fig. 3 B): pyruvate kinase (cytoplasm), histone H1 (nucleus), calnexin (ER membrane), and transferrin receptor (plasma membrane). Fig. 3 B demonstrates that there was virtually no cross-contamination of soluble proteins between C and N, whereas ER and plasma membrane constituents were found in both fractions. However, most importantly LMB treatment did not affect the distribution of any of these membrane marker proteins, indicating that the LMB-induced enrichment of c-erbB-3 in N is independent of the membrane components found in this fraction. Omission of Triton X-100 from the cytoplasmic extract buffer during the preparation of C caused an almost complete disappearance of c-erbB-3–specific immunoreactive material in this fraction as demonstrated by blotting with the C17 antibody (Fig. 3 C, first compared with second lane). Instead, high amounts of c-erbB-3 were recovered from the corresponding Triton X-100–free membrane pellet after centrifugation at 100,000 *g* (Fig. 3 C, third lane). However, a direct quantitative comparison of c-erbB-3 in the membrane pellet and in the Triton X-100–treated cytoplasmic fraction is inappropriate, since an arbitrary amount of the membrane pellet was loaded onto the gel. These data indicate that c-erbB-3 found in fraction C is primarily membrane bound.

Secretion of endogenous HRG

HRG represents the cognate ligand of c-erbB-3 causing heterodimerization of c-erbB-3 with c-erbB-2 and activation of the receptor complex. This growth factor was found to be expressed in mammary tissues. Therefore, serum-free culture

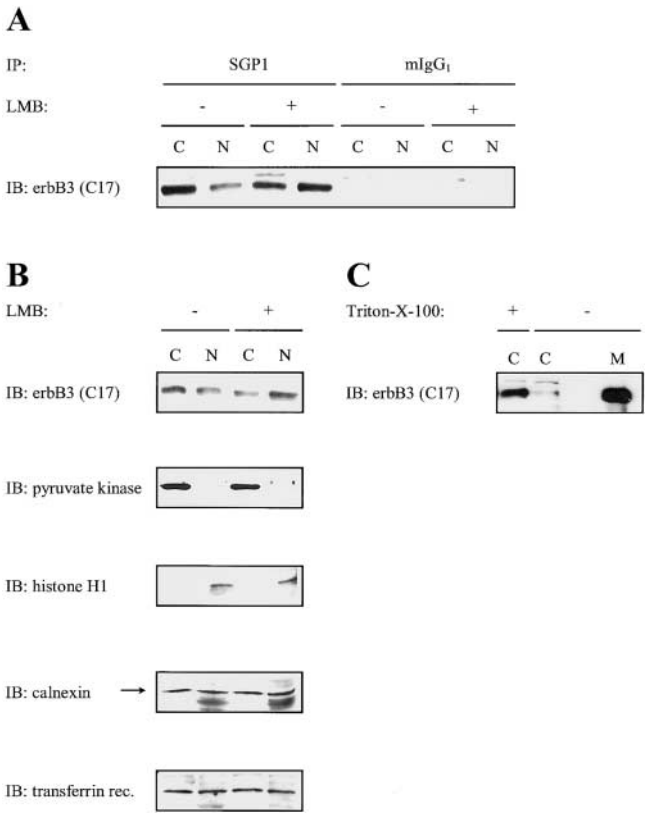

Figure 3. **Immunochemical demonstration of c-erbB-3 in MCF-7 cells.** (A) 400 μg protein from untreated (−) or LMB-treated (+) C or N MCF-7 fractions were immunoprecipitated (IP) with SGP1, which detects an extracellular epitope of c-erbB-3, or with $mIgG_1$ and blotted (IB) with C17, which binds to the cytoplasmic part of c-erbB-3. (B) 20 μg total protein from each fraction (C or N) were blotted with anti–c-erbB-3 (C17), antipyruvate kinase, anti–histone H1, anticalnexin, or antitransferrin receptor. Note calnexin has an apparent molecular mass of 90 kD (arrow). The bottom band seen in N represents a nonspecifically stained bulk nuclear protein. (C) Cytoplasmic-enriched fractions were prepared with or without the addition of 0.2% Triton X-100 and blotted for c-erbB-3 (C17). After centrifugation at 100,000 *g*, an arbitrary amount of the membrane pellet (M) from the fraction prepared without Triton X-100 was loaded as a control.

supernatants from MTSV1-7 and MCF10A cell cultures were tenfold concentrated and subjected to SDS-PAGE followed by immunoblotting for HRG. Fig. 4 demonstrates that confluent monolayers of MTSV1-7 cells but not of MCF10A cells secrete an immunoreactive protein of the expected size (44 kD), indicating that MTSV1-7 cells express endogenous HRG, whereas MCF10A cells do not produce detectable amounts of this growth factor.

Effects of exogenous HRGβ1

We hypothesized that HRG, which profoundly affects c-erbB-3 function, might also regulate its subcellular distribution. It has to be noted that c-erbB-3, although found primarily within the nuclei, was concomitantly seen in variable amounts within the cytoplasm and at the cell membrane as well (Fig. 1 A, b, and B, b–d, Fig. 2 A, Fig. 3, and Tables I and II). This might partially be caused by autocrine activation of c-erbB-3 via endogenous HRG. Permeable filters, in contrast to solid substrate, provide a polarizing environment

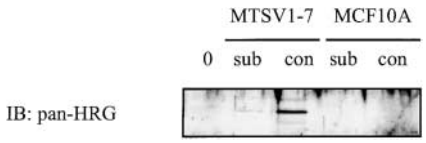

Figure 4. **Immunochemical analysis of HRG secretion from MTSV1-7 and MCF10A cells.** Concentrated serum-free supernatants from cell-free (0), subconfluent (sub), and confluent (con) MTSV1-7 or MCF10A cultures were blotted with anti-pan HRG.

for epithelial cells and caused MTSV1-7 cells not only to differentiate and to develop epithelial polarity as determined by localization of E-cadherin and ZO-1 (unpublished data) and by the presence of microvilli (Fig. 5 C, 24 h) but also to respond to exogenous HRG by a time-dependent export of c-erbB-3 into nonnuclear compartments, which was completed by ~24 h (Fig. 5, A–C). However, under HRG-free conditions (no HRG added and endogenous HRG blocked by anti-HRG) c-erbB-3 was concentrated in the granular component of the nucleoli (Fig. 5 A, 0 min, and C, 0 min) being the site of rRNA processing and preribosome formation. After 1 h of exposure to exogenous HRGβ1, a mixed nucleolar/nuclear staining pattern became evident, and after 4 h a cytoplasmic staining pattern became evident, which was completed by 24 h with no further change upon longer exposure (Fig. 5, A–C). Cells not blocked with anti-HRG exhibited a small amount of cytoplasmic c-erbB-3, which may be caused by endogenous HRG, and responded similarly to exogenous HRGβ1 (Fig. 5 B). Endogenous HRG was below the detection limit of confocal immunofluorescence microscopy in

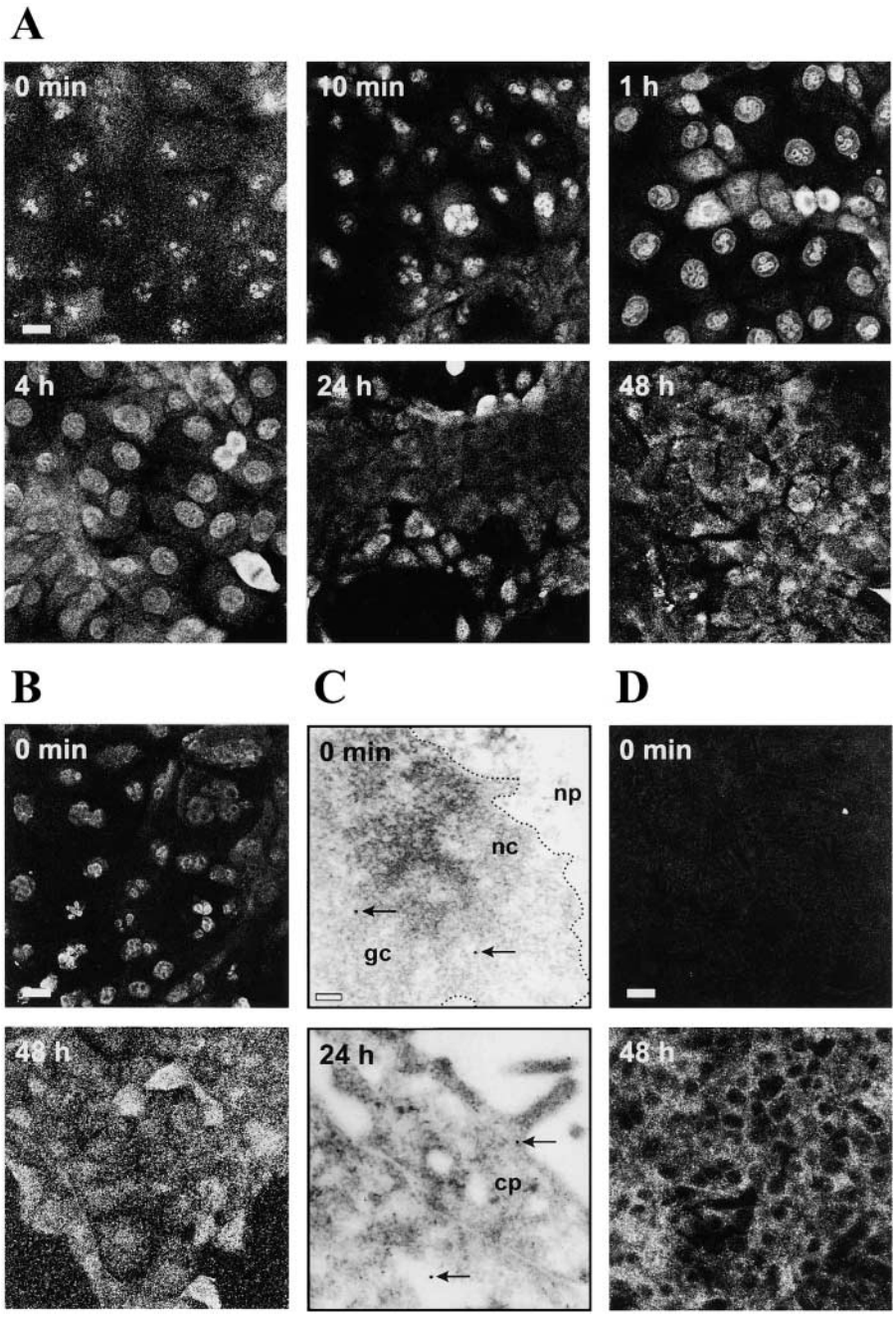

Figure 5. **HRGβ1 affects subcellular distribution of c-erbB-3.** MTSV1-7 were examined by confocal immunofluorescent microscopy (A,B, and D) and immuno EM (C) for c-erbB-3 (A–C) or HRG (D). (A) Cells on filters pretreated with neutralizing anti-HRG (10 μg/ml, 48 h) were exposed for various times to 1 nM HRGβ1. Note mitotic cells were strongly positive. (B) Endogenous HRG was not blocked by anti-HRG (0 min) before exogenous HRGβ1 (1 nM, 48 h). (C) 0 min, after blocking of endogenous HRG, c-erbB-3 (arrows) was found in the granular component (gc) of the nucleolus (nc). np, nucleoplasm. At 24 h, added HRGβ1 (1 nM) caused relocation of c-erbB-3 into the cytoplasm (cp) and to the cell membrane. (D) Cells were treated as in B but immunostained with anti-pan HRG. Bars: (A, B, and D) 40 μm; (C) 0.1 μm.

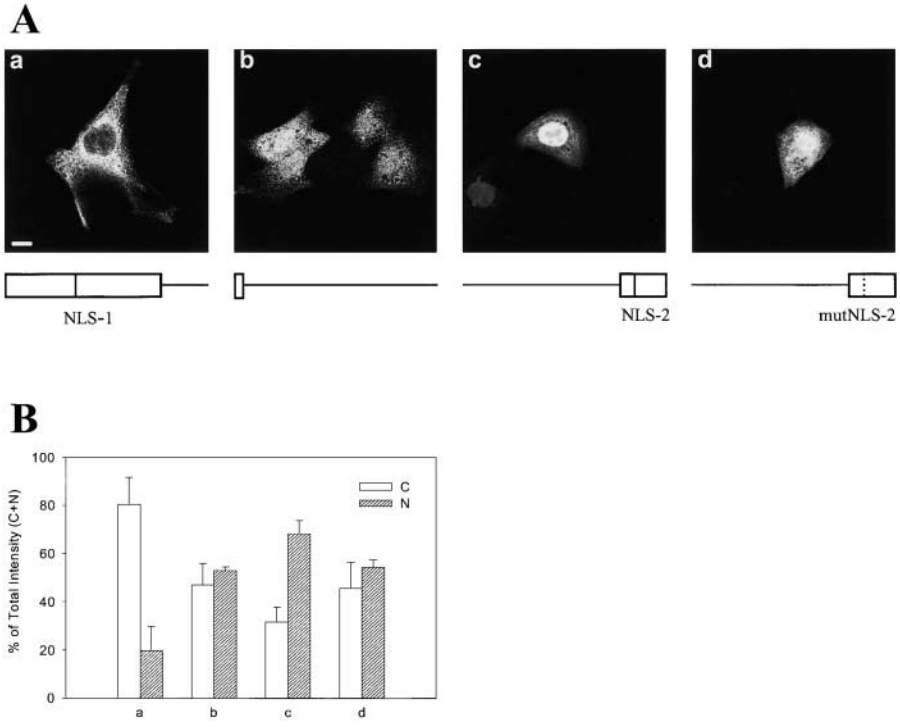

Figure 6. **NLS-2 is functional in c-erbB-3.** (A) MTSV1-7 transiently transfected with EGFP–mutant-erbB-3 fusion constructs. Removal of NLS-2 by COOH-terminal truncation completely precluded nuclear localization of the protein in A, panel a (158 kD; larger than the size exclusion limit of the nuclear pore complex, which is ~60 kD), whereas the smaller construct in A, panel b (36 kD) can be found in both compartments. The COOH-terminal fragment containing NLS-2 (55 kD) is concentrated in the nuclei (A, c). Inactivating mutation of NLS-2 (mutNLS-2) partially reverts nuclear concentration (A, d). Bar, 25 μm. (B) At least four independent points, randomly chosen in each compartment (C, cytoplasm; N, nucleus), were measured in arbitrary units (pixel intensity), and relative antigen staining was expressed for each compartment in percent of total (C + N, means ± SD).

untreated MTSV1-7 cells, whereas added HRGβ1 was seen readily in the cytoplasm but not in the nucleus during the whole observation period of 48 h (Fig. 5 D).

NLS within c-erbB-3

Nuclear localization is usually mediated by specific, short basic amino acid sequences within nuclear proteins (nuclear localization signals [NLSs]). Therefore, we analyzed the c-erbB-3 protein sequence for the presence of such sequences. Using PSORT II software (http://psort.nibb.ac.jp), we identified two potential NLSs within the c-erbB-3 protein (NLS-1, RPRR and NLS-2, RRRR). To directly determine the functional significance of these two NLSs, we ligated different c-erbB-3 cDNA fragments containing either NLS-1 or NLS-2 coding sequences to enhanced green fluorescent protein (EGFP) and transfected them into MTSV1-7 cells. Fig. 6 A, a, demonstrates that the complete NH_2-terminal part of c-erbB-3 containing NLS-1 (amino acids 1–1,088, yielding a 158-kD fusion protein) was unable to target EGFP into the nucleus. Deletion of all but the first 74 amino acids of c-erbB-3 (amino acids 1-74, yielding a 36-kD fusion protein) led to a mixed cytoplasmic and nuclear localization of the construct (Fig. 6 A, b). The size exclusion limit of the nuclear pore complex is ~60 kD. Therefore, nuclear entry of the small fusion protein (36 kD) is most likely caused by passive diffusion through the nuclear pore complexes. In contrast, fusing the COOH terminus of c-erbB-3 containing NLS-2 (amino acids 1,089–1,323) to EGFP yielded a 55-kD protein, which was concentrated in the cell nucleus (Fig. 6 A, c). Semiquantitative analysis of the distribution of the recombinant proteins between the two compartments was done by image analysis as described and shown in Fig. 6 B. Site-directed mutagenesis of NLS-2 (RRRR to RSGR) reduced nuclear localization to levels which were similar to those seen for the 36-kD construct (Fig. 6 A, d compared with b, and 6 B, d compared with b).

Transfer of a sequence containing NLS-2 (RRRRHSP*) of c-erbB-3 to chicken pyruvate kinase (CPK), an exclusively cytoplasmic protein, further confirmed that NLS-2 is responsible for nuclear targeting of c-erbB-3. Confocal immunofluorescence microscopy revealed that transfected wild-type CPK localizes to the cytoplasm of MTSV1-7 cells (Fig. 7 A, CPK). However, fusing the control NLS of human lamin C to CPK causes CPK to enter the nucleus of MTSV1-7 cells (Fig. 7 A, CPK-CoNLS). Most importantly, NLS-2 of human c-erbB-3 (Fig. 7 A, CPK-NLS-2) or the complete COOH terminus of c-erbB-3 (amino acids 1,089–1,323) (Fig. 7 A, CPK-erbB3CT) were as active in targeting CPK to the nucleus of MTSV1-7 cells as the control NLS of human lamin C. Semiquantitative evaluation of the subcellular distribution of these constructs was done by image analysis as described and shown in Fig. 7 B.

Discussion

Spontaneous and LMB-induced nuclear localization of $p185^{c\text{-}erbB\text{-}3}$

This report provides the first evidence that c-erbB-3 can be localized in the nucleus of normal and malignant human mammary epithelial cells. The specific subcellular distribution was independent of the cell fixation procedure and of the individual antibodies used. In particular, nuclear localization of c-erbB-3 was observed in nonmalignant MTSV1-7 cells by confocal immunofluorescence microscopy using one monoclonal (RTJ2) and two different polyclonal antibodies (Ab-9 and C17) directed either against a cytoplasmic epitope located next to the very COOH terminus (C17) or more upstream from it (RTJ2), or against a domain near the NH_2 terminus (Ab-9) of c-erbB-3. These data were further confirmed by immuno EM using RTJ2 and Ab-9 (Fig. 1).

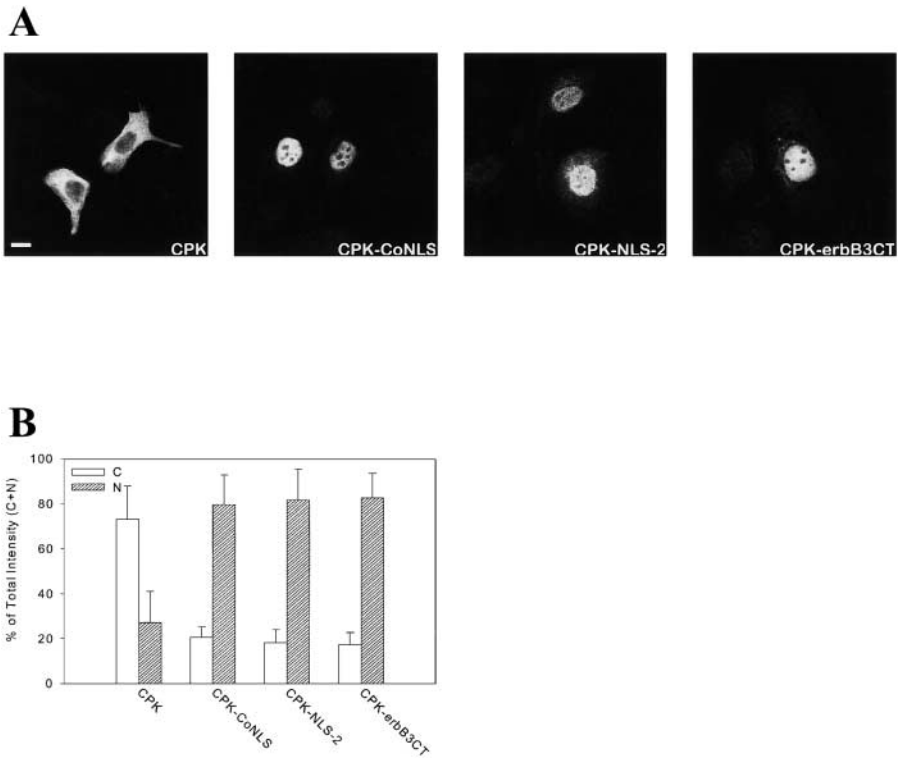

Figure 7. **NLS-2 is sufficient for nuclear targeting.** (A) MTSV1-7 transiently transfected with CPK fusion constructs. CPK alone localizes to the cytoplasm (CPK), whereas the control NLS of human lamin C (CPK-CoNLS) mediates efficient nuclear targeting of CPK. NLS-2 of human c-erbB-3 (CPK-NLS-2), consisting of the sequence RRRRHSP*, efficiently localizes CPK to the nucleus. The same is true for the complete COOH terminus of c-erbB-3 (CPK-erbB3CT). Bar, 25 μm. (B) Quantitation (performed as in 6 B) demonstrated that NLS-2 and the COOH terminus of c-erbB-3 are as effective as the control NLS of human lamin C in directing CPK from the cytoplasm (C) into the nucleus (N).

RTJ2 seemed to detect nuclear c-erbB-3 with higher affinity and specificity than the other antibodies tested. This might be due to a different conformation of nuclear c-erbB-3 when compared with nonnuclear c-erbB-3, thereby better exposing the particular epitope recognized by RTJ2. Therefore, RTJ2 was chosen for the majority of our immunofluorescence experiments. Our data indicate that RTJ2 does not cross-react with some unrelated nuclear bulk protein nor does it selectively detect nuclear c-erbB-3 only. First, nuclear localization of c-erbB-3 was also seen with additional polyclonal antibodies, which recognize unrelated epitopes (Fig. 1, A and B). Second, RTJ2 similarly labeled nonnuclear c-erbB-3 (Fig. 1 B, Fig. 2, BT483, and Fig. 5).

Nuclear staining of variable intensity was also seen in other nonmalignant and malignant human mammary epithelial cells and was found to be strictly dependent on the applied culture conditions. For instance, the nuclear export inhibitor LMB (Fukuda et al., 1997) caused a significant enrichment of c-erbB-3 in the nuclei of cell lines that otherwise revealed only low levels of nuclear staining (Fig. 2 A). A similar effect was observed when MCF-7 cells were transiently transfected with full-length c-erbB-3 tagged with the FLAG peptide followed by LMB treatment and immunofluorescent detection of the receptor using the M2 anti-FLAG antibody (Fig. 2 B). This is in accordance with data obtained by immunoprecipitation and Western blotting of C and N fractions from untreated and LMB-treated MCF-7 cells, which revealed a significant LMB-induced deprivation of c-erbB-3 in C and a concurrent enrichment in N (Fig. 3). Although we cannot entirely exclude that some c-erbB-3 found in the C fraction might come from leakage of the receptor from the nucleus during cell lysis and fractionation, several lines of evidence yet argue against this. First, analysis of the purity of the fractions revealed that there was virtually no cross-contamination of soluble proteins between C and N as indicated by the distribution of the nuclear protein histone H1 and the cytoplasmic marker pyruvate kinase (Fig. 3 B). Second, the data in Fig. 3 C demonstrate that "cytoplasmic" c-erbB-3 is primarily membrane bound in MCF-7 cells. Moreover, it is important to note that LMB did not affect the distribution of the membrane marker proteins calnexin and transferrin receptor between C and N, although it still caused cytoplasmic deprivation and nuclear accumulation of c-erbB-3, indicating that contaminating membrane components are not a major source for the presence of c-erbB-3 in N. Interestingly, the molecular mass of nuclear c-erbB-3 was ~185 kD. Thus the nuclear species represents the full-length protein and not a truncated version of c-erbB-3.

Although cell surface labeling for c-erbB-3 was rather weak in immunofluorescence microscopy, flow cytometry clearly demonstrated that c-erbB-3 can be detected in the plasma membrane. Despite general paucity of reports on the subcellular distribution of c-erbB receptors, there is one paper (Xie and Hung, 1994) describing partial nuclear localization of low levels of c-neu, the rat homologue of human c-erbB-2, in rat DHFR/G8 cells. Another study (Srinivasan et al., 2000) demonstrated nuclear localization of c-erbB-4 in primary human breast cancers, which might be caused by a potential NLS within the c-erbB-4 amino acid sequence. These data are supported by a very recent report from Ni et al. (2001), who demonstrated that the intracellular domain of c-erbB-4 gets cleaved by γ-secretase. The truncated cytoplasmic fragment then translocates into the nucleus (Ni et al., 2001). In addition, Lin et al. (2001) reported nuclear localization of c-erbB-1 in several malignant cell lines and presented evidence suggesting that nuclear c-erbB-1 might function as a transcription factor. In contrast to c-erbB-4 but in accordance with our data on c-erbB-3 nuclear c-erbB-1

was found to be the full-length receptor and not a truncated version (Lin et al., 2001; Bourguignon et al., 2002).

Although the list of nuclear localization of transmembrane receptors is considerably long and includes the interleukin-1 receptor (Curtis et al., 1990), the NGF receptor (Rakowicz-Szulczynska et al., 1988), the growth hormone receptor (Lobie et al., 1994), and several endocytosis-related proteins (Vecchi et al., 2001), one of the most well-known examples is the nuclear translocation of the FGF receptor in response to various stimuli (Maher, 1996; Stachowiak et al., 1996). The lack of a clearly understood potential pathway for nuclear import of full-length transmembrane growth factor receptors has raised some concerns about the relevance of nuclear growth factor receptors (Oksvold et al., 2002). However, a recent report demonstrated physical interaction of the FGF receptor with the nuclear import factor importin β (Reilly and Maher, 2001), suggesting that nuclear import of the FGF receptor occurs via the importin β pathway. Although we have no clear indication about potential nuclear import pathways for c-erbB-3, we consider a similar pathway at least possible.

Furthermore, it is evident that several polypeptide growth factors can enter the cell nucleus (Keresztes and Boonstra, 1999). Correspondingly, FGF-3 was found to localize to the cell nucleus, and an NLS was identified in the protein (Antoine et al., 1997). Using the PSORT II software (http://psort.nibb.ac.jp), we found a potential NLS near the NH_2 terminus (NLS-1) and the COOH terminus (NLS-2) of the c-erbB-3 sequence. Reinhardt's method (Reinhardt and Hubbard, 1998) for cytoplasmic/nuclear discrimination predicted nuclear localization for c-erbB-3 with a reliability of 70%. Therefore, we constructed EGFP–mutant erbB-3 fusion proteins and found that a tetra arginine repeat near the COOH terminus of c-erbB-3 (NLS-2) was able to target EGFP to the nucleus, whereas a similar potential NLS (NLS-1) near the NH_2 terminus of c-erbB-3 was inactive (Fig. 6). Furthermore, transfer of NLS-2 to CPK, an exclusively cytoplasmic protein (Frangioni and Neel, 1993), resulted in efficient nuclear targeting of the fusion protein (Fig. 7). These data clearly indicate that NLS-2 itself is sufficient to confer nuclear targeting to heterologous proteins different from c-erbB-3. Besides that, the c-erbB-3 sequence (Kraus et al., 1989) contains several leucine-rich domains, which fulfill the formal requirements for CRM1-dependent nuclear export signals, and we observed that the CRM1 inhibitor LMB (Fukuda et al., 1997) can trap endogenous c-erbB-3 in the nuclei of several different malignant and nonmalignant cell lines of mammary epithelial origin, supporting the idea that nuclear localization represents a general property of c-erbB-3 and is not restricted to a specific cell line. Additionally, we were able to demonstrate LMB-induced nuclear accumulation of a transiently transfected c-erbB-3–FLAG fusion protein. In the past, nuclear localization of c-erbB-3 might have been overlooked in many cell lines due to prominent cytoplasmic staining caused by active nuclear export. The use of LMB allowed to selectively stop this export and thus enabled visualization of c-erbB-3 in the nuclei of several cell lines. In the absence of LMB, nuclear staining for c-erbB-3 was most intense in BT20 and MDA468 cells and could not be further enhanced by LMB, indicating that nuclear export pathways are not very active in these cells.

Epithelial cell polarity and subnuclear localization of c-erbB-3

In contrast to solid substrate culture, MTSV1-7 grown on permeable filters polarized and differentiated as determined by localization of E-cadherin and ZO-1 (unpublished data) and by the presence of microvilli (Fig. 5 C), which was accompanied by concentration of c-erbB-3 in the nucleoli, where ribosome biosynthesis occurs, including transcription of ribosomal genes and assembly of the ribosome subunits (Shaw and Jordan, 1995). Previous studies showed that growth factors like FGFs and parathyroid hormone–related peptide can enter the nucleolus (Pederson, 1998). However, to our knowledge no transmembrane growth factor receptor has ever been observed within the nucleolus.

Effect of endogenous and exogenous HRG on the subcellular distribution of c-erbB-3

A previous report demonstrated that primary human mammary epithelial cells express large amounts of HRG (Aguilar et al., 1999). We examined immortalized nonmalignant MTSV1-7 and MCF10A human mammary epithelial cells for secretion of HRG and found it in one of them (MTSV1-7) (Fig. 4). HRG is the cognate ligand for c-erbB-3 and might affect its subcellular distribution in an autocrine and/or paracrine fashion. Therefore, we blocked secreted HRG with a neutralizing antibody, which caused nucleolar confinement of c-erbB-3 in MTSV1-7 grown on filters. Conversely, exogenous HRGβ1 caused export of c-erbB-3 from the nucleolus into the nucleoplasm and then into the cytoplasm. In contrast to a previous report demonstrating that HRG contains a potential NLS and is transported into the nucleus of the breast cancer cell line SKBR-3 (Li et al., 1996), we found that neither endogenous nor exogenous HRG enters the nucleus of nonmalignant MTSV1-7 cells (Fig. 5 D). These data led us to suppose that HRG induces nucleolar and nuclear export of c-erbB-3 by anchoring it to nonnuclear structures, thus leading to a slow enrichment of c-erbB-3 in the cytoplasm and its deprivation in the nucle(ol)us. Although the exact mechanisms controlling the equilibrium between nucle(ol)ar and nonnucle(ol)ar c-erbB-3 are still unknown, it still appears that HRG is crucial in determining its balance by binding it outside the nucleus not allowing its reentry. Interestingly, four tumor cell lines (MCF-7, BT474, T47D, and BT483) spontaneously exhibited low levels of nuclear c-erbB-3, whereas two others (BT20 and MDA468) and two nonmalignant cell lines (MTSV1-7 and MCF10A) revealed strong nuclear staining, possibly reflecting different activation states of the c-erbB-3 pathway. Many breast cancer cells exhibit overexpression/hyperactivation of c-erbB-2, which is the major heterodimer partner of c-erbB-3 and plays a crucial role in controlling c-erbB-3 activation and maybe subcellular localization. Accordingly, MDA468 are negative for c-erbB-2 and thus devoid of c-erbB-2/-3 heterodimers. On the other hand, BT20 cells overexpress c-erbB-1, which competes with c-erbB-3 for heterodimerization with c-erbB-2. It is thus very likely that these cells are also very poor in active c-erbB-2/-3 heterodimers. Strikingly,

c-erbB-2 was invariably expressed in the cytoplasm and the membrane, irrespective of stage of malignancy, the level of baseline expression, and the culture conditions (unpublished data), indicating that the subcellular distribution of c-erbB-3 is specific for this particular receptor.

Although the ultimate mechanisms of nucleocytoplasmic shuttling of c-erbB-3 and its precise role in the nucleus remain to be elucidated, our data open up new perspectives on the functions of c-erbB proteins. Together, c-erbBs may not only represent membrane-anchored signal transducers with crucial roles in malignant transformation and progression, but as constituents of nucleolar structures they might also regulate ribosome biosynthesis.

Materials and methods

Cell culture

The MTSV1-7 nonmalignant human mammary epithelial cell line (a gift from Dr. J. Taylor-Papadimitriou, Imperial Cancer Research Fund, London, UK) was maintained in DME supplemented with 10% FCS, 100 IU (μg)/ml penicillin-streptomycin, 2 mM glutamine, 10 μg/ml insulin (GIBCO BRL), and 5 μg/ml hydrocortisone (Sigma-Aldrich). The human breast cancer cell lines MCF-7, BT474, T47D, MDA468, and BT20 (American Type Culture Collection) were cultivated in DME containing 10% FCS, 100 IU (μg)/ml penicillin-streptomycin, and 2 mM glutamine (standard medium). BT483 cells (American Type Culture Collection) were grown in standard medium containing an additional 10 μg/ml insulin, whereas MCF10A nonmalignant human mammary epithelial cells (American Type Culture Collection) were maintained in serum-free MEGM (Clonetics) according to the manufacturer's instructions.

LMB treatments

For immunofluorescence, cells were seeded at $10^4/cm^2$ into 8-well glass chamber slides (Nunc) and allowed to settle for 24 h. Media were replaced, and 20 ng/ml LMB (a gift from Dr. B. Wolff-Winiski, Novartis, Vienna, Austria) in 0.1% methanol or solvent alone were added to the cells and incubated for 24 h. c-erbB-3–FLAG–transfected MCF-7 cells were treated for 24 h with 5 ng/ml LMB or solvent.

For fractionation experiments, MCF-7 cells were seeded into five 500-cm^2 plates and grown to 80% confluence. 5 ng/ml LMB was added to three of the plates, whereas the remaining plates were treated with 0.1% methanol for 24 h. These conditions were found previously to yield optimal nuclear localization of c-erbB-3 in MCF-7 cells, whereas toxicity was kept at a minimum (unpublished data).

Flow cytometry

MCF-7, MDA468, T47D, and BT20 cells were rinsed with PBS, briefly trypsinized, and washed with FACS® buffer (1% BSA, 0.1% NaN_3 in PBS). All subsequent incubations and washings were performed in this buffer. Labeling with 10 μg/ml of mouse monoclonal anti–c-erbB-3 antibody (SGP1; Neomarkers) or irrelevant control mIgG (Dako) was performed for 30 min on ice. Washed cells were then labeled for 30 min on ice with goat anti–mouse Ig-Alexa488 (1:200; Molecular Probes). Analysis was performed with a FACScan® (Becton Dickinson) equipped with CellQuest software. For life gating, propidium iodide (0.5 μg/ml; Sigma-Aldrich) was added to the cold cells immediately before measurement, and 5×10^3 nonpermeable cells per sample were measured. Results were expressed as mean fluorescence intensity.

Nuclear and cytoplasmic fractions

Control and LMB-treated MCF-7 were washed twice with PBS, harvested by scraping and centrifuged (1,850 *g*, 10 min, 4°C), suspended in 5 packed cell vol hypotonic buffer (10 mM Hepes, pH 7.9, 1.5 mM $MgCl_2$, 10 mM KCl, 0.2 mM PMSF, 0.5 mM DTT, protease inhibitors [1 tablet Complete® EDTAfree/50 ml, Roche]), recentrifuged, resuspended in 3 packed cell vol hypotonic buffer, incubated on ice (10 min), homogenized (Dounce, type B pestle, 25 strokes), and spun (3,300 *g*, 15 min, 4°C). The supernatant was designated S1 and saved. The nuclear pellet was washed twice with 10 ml hypotonic buffer and suspended in 0.5 packed nuclear vol low salt buffer (20 mM Hepes, pH 7.9, 25% glycerol, 1.5 mM $MgCl_2$, 20 mM KCl, 1 mM EGTA, 0.2 mM PMSF, 0.5 mM DTT, 0.2% Triton X-100, 1 tablet Complete® Mini EDTAfree/10 ml). Then, 0.5 packed nuclear vol high salt buffer (low salt buffer with 1.2 M KCl) were added, and nuclei were homogenized (25 strokes), extracted on a shaker (30 min, 4°C), and spun (25,000 *g*, 30 min, 4°C). 1 U/ml α_2-macroglobulin (Roche), which is unable to pass a 10-kD-cutoff dialysis membrane, was added to the supernatant and dialyzed (dialysis buffer [DB]; 20 mM Hepes, pH 7.9, 10% glycerol, 300 mM KCl, 0.5 mM EGTA, 0.2 mM PMSF, 0.2% Triton X-100; 1 h, 4°C) in a slide-a-lyzer cassette (MWCO 10000; Pierce Chemical Co.). The dialyzed nuclear extract was recentrifuged (25,000 *g*, 20 min, 4°C), aliquoted, and stored at −80°C.

Cytoplasmic extracts. Saved supernatant S1 was mixed with 0.11 vol 10× cytoplasmic extract buffer (300 mM Hepes, pH 7.9, 30 mM $MgCl_2$, 1.4 M KCl, 2% Triton X-100), spun (100,000 *g*, 1 h, 4°C; S100 fraction), and α_2-macroglobulin was added before dialysis. The dialyzed fraction was centrifuged (25,000 *g*, 20 min, 4°C) and stored as above.

For some experiments a simplified protocol was used. The supernatant S1 was divided into 2 aliquots, and cytoplasmic extract buffer with or without Triton X-100 was added before centrifugation at 100,000 *g*. The supernatants were subjected to protein assay according to Bradford and used directly for Western blotting. The membrane pellet from the fraction without Triton X-100 was dissolved by boiling (5 min, 95°C) in 400 μl Laemmli buffer, and insoluble components were removed by centrifugation before 10 μl of this solution was used for Western blotting.

Immunoprecipitation

Concentration of nuclear and cytoplasmic protein (400 μg each) from LMB-treated or untreated MCF-7 cells was balanced with DB, which was supplemented with 1 tablet Complete® Mini EDTAfree/10 ml (DBC). Gamma bind plus sepharose beads (Amersham Pharmacia Biotech) were washed and resuspended to original vol with DBC. 10 μl beads, 4 μg anti–c-erbB-3 (SGP1; Neomarkers) or murine IgG1 (Dako), and respective fraction (400 μg protein) were mixed, incubated on a shaker (1 h, 4°C), washed five times (200 μl DBC), spun (10,000 *g*, 1 min, 4°C), resuspended in Laemmli buffer, boiled (5 min), and stored frozen.

Western blotting

Proteins were separated by 7.5% SDS-PAGE, and gels were equilibrated for 30 min in blotting buffer (20% methanol, 380 mM glycine, 50 mM Tris, 0.1% SDS). Proteins were blotted onto polyvinylidene difluoride membranes (New England Nuclear), which were then blocked for 1 h in 5% BSA/PBS at room temperature (RT), washed with PBS containing 0.1% Tween 20 (PBST), and immunostained for 3 h at RT in 1% BSA/PBS containing the primary antibody: polyclonal anti–c-erbB-3 (0.2 μg/ml, C17; Santa Cruz Biotechnology, Inc.), polyclonal anti-CPK (cross-reactive with human pyruvate kinase) (1:4,000; Convance), monoclonal anti–histone H1 (0.2 μg/ml; Neomarkers), monoclonal anti-calnexin (1:400; Affinity BioReagents, Inc.), or monoclonal antitransferrin receptor (1 μg/ml; Neomarkers). Washed blots were labeled for 1 h with sheep anti–mouse or donkey anti–rabbit Ig F(ab')$_2$-HRP conjugate (1:10,000 in 1% BSA/PBST; Amersham Pharmacia Biotech), washed extensively in PBST, immersed in ECL detection reagent (New England Nuclear), and exposed to X-Omat AR film (Eastman Kodak Co.).

For the detection of secreted HRG, MTSV1-7 and MCF10A cells were grown in serum-free MEGM. Conditioned culture supernatants were then recovered and 10-fold concentrated with Centricon 10 concentrators (Millipore). 10 μl Laemmli buffer were added to 10 μl of the concentrates and boiled (5 min), separated by 10% SDS-PAGE, blotted, and immunostained with 1 μg/ml rabbit anti-HRG (Ab-2; Neomarkers) and donkey anti–rabbit Ig F(ab')$_2$-HRP conjugate (1:10,000; Amersham Pharmacia Biotech) as above.

Immunofluorescence (c-erbB, FLAG, and HRG)

Washed cells (PBS) were fixed in 2% paraformaldehyde (PFA) (5 min, RT), permeabilized in methanol/acetone (1:1, 3 min, −20°C), air dried, and stored at −80°C. Before use, cells were rehydrated in PBS (5 min, RT), blocked in 5% sheep serum/PBS (30 min, RT), and washed again. Antibodies (in 5% sheep serum/PBS, 1 h, RT) were against c-erbB-2 (10 μg/ml mouse monoclonal mAB-3; Oncogene Research Products), c-erbB-3 (10 μg/ml mouse monoclonal RTJ2; Neomarkers) (5 μg/ml rabbit polyclonal C17; Santa Cruz Biotechnology, Inc.) (10 μg/ml rabbit polyclonal Ab-9; Neomarkers), FLAG (20 μg/ml, mouse monoclonal M2; Sigma-Aldrich), and HRGβ (10 μg/ml goat polyclonal C18; Santa Cruz Biotechnology, Inc.). Secondary antibodies were goat anti–mouse or goat anti–rabbit Ig-Alexa488 or donkey anti–goat Ig-Alexa546 (1:200 in 5% sheep serum/PBS, 30 min, RT; Molecular Probes). Washed cells were embedded in Prolong Antifade (Molecular Probes) and evaluated in an LSM400 confocal microscope (ZEISS) with a thickness of the optical sections of 0.8 μm.

Immunofluorescence (CPK)

For detection of CPK fusion proteins, fixed cells were quenched in 50 mM glycine/PBS (5 min, RT). Blocking was performed with 10% goat serum in PBS containing 0.2% NP-40 (30 min, RT). All subsequent washing and incubation steps were performed as above in solutions containing 0.2% NP-40 to suppress background staining caused by cross-reactivity of the antiserum with endogenous (human) pyruvate kinase (Frangioni and Neel, 1993).

The following antibodies were used: crude rabbit antiserum against CPK (Convance, 1:500) and goat anti–rabbit Ig-Alexa488 (1:200; Molecular Probes).

Filter assay

MTSV1-7 cells were plated at 10^5 into 25 mm Anopore-Inserts (Nunc). Neutralizing anti-HRG (Ab-2, 10 μg/ml; Neomarkers) was added where indicated. After 48 h, cells were washed and exposed for the indicated times to 1 nM recombinant HRGβ1 (Neomarkers). Filters were broken out at the end of the experiments, cut, and processed as above.

Immuno EM

MTSV1-7 grown in culture flasks were fixed with 2.5% PFA/0.5% glutaraldehyde in 0.1 M Soerensen buffer (SB; 30 min, 4°C) and washed 3 × 10 min with SB. Two batches of MTSV1-7 grown on filter were prepared: one treated with neutralizing anti-HRG and one with subsequent exposition to 1 nM HRGβ1 for 24 h. Small pieces of filters were fixed with 4% PFA/0.5% glutaraldehyde in 0.1 M SB (30 min, 4°C) and washed three times with SB. Filters and MTSV1-7 in suspension were embedded in the hydrophilic resin LRWhite (London Resin Company). Ultrathin sections of MTSV1-7 cells were mounted on meshed gold grids; sections of the filters were mounted on Formvar-coated gold grids.

Grids were preincubated in PBS plus 1% BSA plus 1% normal goat serum, pH 7.4 (PBSB; 30 min, RT), incubated overnight with anti–c-erbB-3 (monoclonal RTJ2, 10 μg/ml in PBSB, and rabbit polyclonal Ab-9, 5 μg/ml in PBSB; 4°C), washed thoroughly in PBST, pH 7.4 and 8.2, labeled with 10 nm gold-conjugated goat anti–mouse or goat anti–rabbit IgG (1:40 in PBSB, pH 8.2; British BioCell), and washed in PBST, pH 8.2, and in distilled water. Contrast was enhanced with 2% aqueous uranyl acetate (30 min), and sections were evaluated with a Jeol EM1200 electron microscope equipped with a digital camera (BioScan 792; Gatan). For controls, the primary antibody was omitted. Signal distribution over cytoplasm and nucleus was quantified by counting gold particles per respective area in 10 randomly chosen cells per sample. The area was measured with the help of morphometry software (KS400; Kontron). For statistical comparison of datasets of RTJ2, Ab-9 and control series Student's *t* test was applied. Normal (Gaussian) distribution of datasets was checked using the R/s test.

EGFP fusion protein construction and analysis

A plasmid containing full-length c-erbB-3 was linearized by complete XbaI digestion, and the signal peptide was removed by partial SmaI digestion. pEGFP-C1 (CLONTECH Laboratories, Inc.) was digested with Ecl136II and XbaI before ligation.

Two COOH-terminal deletion mutants of the c-erbB-3 cDNA were constructed by cleaving the c-erbB-3 insert at the unique Ecl136II and XbaI or the EcoRI and XbaI restriction sites. The EcoRI and XbaI sites of c-erbB-3 and pEGFP-C1 were then filled in, respectively, and the COOH-terminally truncated c-erbB-3 inserts were ligated with the pEGFP-C1 vector. This yielded proteins with EGFP fused to amino acids 1–1,088 (Ecl136II) or 1-74 (EcoRI) of c-erbB-3.

In addition, the COOH terminus of c-erbB-3 was fused to EGFP using the Ecl136II site of c-erbB-3, the filled-in HindIII site of pEGFP-C1 and the XbaI sites of both vector and insert, yielding a construct containing amino acids 1,089–1,323 of c-erbB-3 downstream of EGFP. Site-specific mutagenesis (R1184S/R1185G) of the latter construct was done with the Quick-Change kit (Stratagene) according to the manufacturer's protocol using the following oligonucleotides: 5′-GGTGGACTGTGCCTTCCGCTCCGGTTCATGTATTC-3′ and 5′-GAATACATGAACCGGAGCGGAAGGCACAGTCCACC-3′. Presence of the double mutation was verified by sequencing.

MTSV1-7 cells were seeded and transfected using Effectene (QIAGEN) adhering to manufacturer's protocols. 24 h after transfection, cells were washed, fixed with 2% PFA as above, embedded in Mowiol/DABCO, and evaluated by confocal microscopy as described above.

FLAG fusion protein construction and analysis

A vector containing full-length c-erbB-3 (supplied by F. Wouters, European Molecular Biology Laboratory, Heidelberg, Germany) was used in order to fuse the FLAG peptide to the COOH terminus of c-erbB-3. The sequence coding for the FLAG peptide was supplied using the following oligonucleotides: 5′-CGACTACAAGGACGACGATGACAAGTGAGCTCGC-3′ and 5′-GGCCGCGAGCTCACTTGTCATCGTCGTCCTTGTAGTCGAT-3′, which were dissolved at 200 μM in 10 mM Tris/HCl, 150 mM NaCl, pH 7.5, and mixed in equal volumes. Annealing was performed by heating the mixture to 94°C and cooling it down to 25°C over a period of 1 h before ligation to c-erbB-3. MCF-7 cells were seeded and transfected using Fugene6 (Roche) according to the supplied protocol. 1 d after transfection, cells were subjected to LMB treatment. Immunofluorescence microscopy was performed as described above.

CPK fusion protein construction and analysis

The p3PK vector, which was used to create fusion proteins of CPK with various human c-erbB-3 fragments, and a positive control plasmid for nuclear localization containing CPK fused to the heterologous NLS of human lamin C (p3PK-NLS-Lamin C) were supplied by Dr. J. V. Frangioni (Beth Israel Deaconess Medical Center, Boston, MA). The sequence coding for NLS-2 of c-erbB-3 (RRRRHSP*) was cloned using the following oligonucleotides: 5′-GATCCCGGAGGAGAAGGCACAGTCCATGAG-3′ and 5′-AATTCTCATGGACTGTGCCTTCTCCTCCGG-3′, which were annealed as above. Using standard procedures, this dsDNA was then ligated to p3PK, which had been digested with EcoRI and BamHI in order to yield a CPK-NLS-2 fusion protein.

Another construct was produced by digesting p3PK with BamHI, filling in, redigesting with XbaI, and dephosphorylation. The insert (COOH-terminal end of c-erbB-3, amino acids 915–1,323) was prepared by digesting c-erbB-3 with BglII, filling in, and redigesting with XbaI. Ligation was performed as above, yielding a construct of CPK fused to the COOH terminus (amino acids 915–1,323) of c-erbB-3 (CPK-erbB3CT). Transfection of MTSV1-7 cells with Effectene and immunofluorescence microscopy were performed as described above.

We thank Drs. J. Taylor-Papadimitriou for the MTSV1-7 cell line, B. Wolff-Winiski for LMB, J.V. Frangioni for p3PK and p3PK-NLS-lamin C, F. Wouters for c-erbB-3-EGFP, and C.D. Roskelley for the critical reading of this article. We acknowledge A. Atzberger for technical assistance concerning flow cytometry and Dr. P.I. Bastiaens for his permission to complete this work in his laboratory.

This work was supported by a grant from the Austrian Science Fund (FWF, P13622-GEN) and the Austrian National Bank (ONB, 7503) to T.W. Grunt.

Submitted: 10 September 2001
Revised: 12 February 2002
Accepted: 17 April 2002

References

Aguilar, Z., R.W. Akita, R.S. Finn, B.L. Ramos, M.D. Pegram, F.F. Kabbinavar, R.J. Pietras, P. Pisacane, M.X. Sliwkowski, and D.J. Slamon. 1999. Biologic effects of heregulin/neu differentiation factor on normal and malignant human breast and ovarian epithelial cells. *Oncogene.* 18:6050–6062.

Alimandi, M., A. Romano, M.C. Curia, R. Muraro, P. Fedi, S.A. Aaronson, P.P. Di-Fiore, and M.H. Kraus. 1995. Cooperative signaling of ErbB3 and ErbB2 in neoplastic transformation and human mammary carcinomas. *Oncogene.* 10:1813–1821.

Antoine, M., K. Reimers, C. Dickson, and P. Kiefer. 1997. Fibroblast growth factor 3, a protein with dual subcellular localization, is targeted to the nucleus and nucleolus by the concerted action of two nuclear localization signals and a nucleolar retention signal. *J. Biol. Chem.* 272:29475–29481.

Bartek, J., J. Bartkova, N. Kyprianou, E.N. Lalani, Z. Staskova, M. Shearer, S. Chang, and J. Taylor-Papadimitriou. 1991. Efficient immortalization of luminal epithelial cells from human mammary gland by introduction of simian virus 40 large tumor antigen with a recombinant retrovirus. *Proc. Natl. Acad. Sci. USA.* 88:3520–3524.

Bourguignon, L., K.-H. Lan, P. Singleton, S.-Y. Lin, D. Yu, and M.-C. Hung. 2002. Localizing the EGF receptor-Reply. *Nat. Cell Biol.* 4:E22–E23.

Curtis, B.M., M.B. Widmer, P. deRoos, and E.E. Qwarnstrom. 1990. IL-1 and its receptor are translocated to the nucleus. *J. Immunol.* 144:1295–1303.

Frangioni, J.V., and B.G. Neel. 1993. Use of a general purpose mammalian expression vector for studying intracellular protein targeting: identification of critical residues in the nuclear lamin A/C nuclear localization signal. *J. Cell Sci.* 105:481–488.

Fukuda, M., S. Asano, T. Nakamura, M. Adachi, M. Yoshida, M. Yanagida, and E. Nishida. 1997. CRM1 is responsible for intracellular transport mediated by the nuclear export signal. *Nature.* 390:308–311.

Grunt, T.W., and H. Huber. 1994. The family of c-erbB genes: from basic research to clinical oncology. *Onkologie.* 17:346–357.

Guy, P.M., J.V. Platko, L.C. Cantley, R.A. Cerione, and K.L. Carraway. 1994. Insect cell-expressed p180erbB3 possesses an impaired tyrosine kinase activity. *Proc. Natl. Acad. Sci. USA.* 91:8132–8136.

Keresztes, M., and J. Boonstra. 1999. Import(ance) of growth factors in(to) the nucleus. *J. Cell Biol.* 145:421–424.

Kraus, M.H., W. Issing, T. Miki, N.C. Popescu, and S.A. Aaronson. 1989. Isolation and characterization of ERBB3, a third member of the ERBB/epidermal growth factor receptor family: evidence for overexpression in a subset of human mammary tumors. *Proc. Natl. Acad. Sci. USA.* 86:9193–9197.

Kraus, M.H., P. Fedi, V. Starks, R. Muraro, and S.A. Aaronson. 1993. Demonstration of ligand-dependent signaling by the erbB-3 tyrosine kinase and its constitutive activation in human breast tumor cells. *Proc. Natl. Acad. Sci. USA.* 90:2900–2904.

Kudo, N., N. Matsumori, H. Taoka, D. Fujiwara, E.P. Schreiner, B. Wolff, M. Yoshida, and S. Horinouchi. 1999. Leptomycin B inactivates CRM1/exportin 1 by covalent modification at a cysteine residue in the central conserved region. *Proc. Natl. Acad. Sci. USA.* 96:9112–9117.

Kumar, R., H.M. Shepard, and J. Mendelsohn. 1991. Regulation of phosphorylation of the c-erbB-2/HER2 gene product by a monoclonal antibody and serum growth factor(s) in human mammary carcinoma cells. *Mol. Cell. Biol.* 11:979–986.

Lemoine, N.R., D.M. Barnes, D.P. Hollywood, C.M. Hughes, P. Smith, E. Dublin, S.A. Prigent, W.J. Gullick, and H.C. Hurst. 1992. Expression of the ERBB3 gene product in breast cancer. *Br. J. Cancer.* 66:1116–1121.

Li, W., J.W. Park, A. Nuijens, M.X. Sliwkowski, and G.A. Keller. 1996. Heregulin is rapidly translocated to the nucleus and its transport is correlated with c-myc induction in breast cancer cells. *Oncogene.* 12:2473–2477.

Lin, S.-Y., K. Makino, W. Xia, A. Matin, Y. Wen, K.Y. Kwong, L. Bourguignon, and M.-C. Hung. 2001. Nuclear localization of EGF receptor and its potential new role as a transcription factor. *Nat. Cell Biol.* 3:802–808.

Lobie, P.E., T.J. Wood, C.M. Chen, M.J. Waters, and G. Norstedt. 1994. Nuclear translocation and anchorage of the growth hormone receptor. *J. Biol. Chem.* 269:31735–31746.

Maher, P.A. 1996. Nuclear translocation of fibroblast growth factor (FGF) receptors in response to FGF-2. *J. Cell Biol.* 134:529–536.

Ni, C.-Y., M.P. Murphy, T.E. Golde, and G. Carpenter. 2001. Gamma-secretase cleavage and nuclear localization of ErbB-4 receptor tyrosine kinase. *Science.* 294:2179–2181.

Oksvold, M., H. Huitfeldt, E. Stang, and I. Madshus. 2002. Localizing the EGF receptor. *Nat. Cell Biol.* 4:E22.

Osherov, N., A. Gazit, C. Gilon, and A. Levitzki. 1993. Selective inhibition of the epidermal growth factor and HER2/neu receptors by tyrphostins. *J. Biol. Chem.* 268:11134–11142.

Pederson, T. 1998. Growth factors in the nucleolus? *J. Cell Biol.* 143:279–281.

Pinkas-Kramarski, R., L. Soussan, H. Waterman, G. Levkowitz, I. Alroy, L. Klapper, S. Lavi, R. Seger, B.J. Ratzkin, M. Sela, et al. 1996. Diversification of Neu differentiation factor and epidermal growth factor signaling by combinatorial receptor interactions. *EMBO J.* 15:2452–2467.

Prigent, S.A., N.R. Lemoine, C.M. Hughes, G.D. Plowman, C. Selden, and W.J. Gullick. 1992. Expression of the c-erbB-3 protein in normal human adult and fetal tissues. *Oncogene.* 7:1273–1278.

Rajkumar, T., and W.J. Gullick. 1994. A monoclonal antibody to the human c-erbB3 protein stimulates the anchorage-independent growth of breast cancer cell lines. *Br. J. Cancer.* 70:459–465.

Rakowicz-Szulczynska, E.M., M. Herlyn, and H. Koprowski. 1988. Nerve growth factor receptors in chromatin of melanoma cells, proliferating melanocytes, and colorectal carcinoma cells in vitro. *Cancer Res.* 48:7200–7206.

Reilly, J.F., and P.A. Maher. 2001. Importin beta-mediated nuclear import of fibroblast growth factor receptor: role in cell proliferation. *J. Cell Biol.* 152:1307–1312.

Reinhardt, A., and T. Hubbard. 1998. Using neural networks for prediction of the subcellular location of proteins. *Nucleic Acids Res.* 26:2230–2236.

Riese, D.J., Y. Bermingham, T.M. van-Raaij, S. Buckley, G.D. Plowman, and D.F. Stern. 1996. Betacellulin activates the epidermal growth factor receptor and erbB-4, and induces cellular response patterns distinct from those stimulated by epidermal growth factor or neuregulin-beta. *Oncogene.* 12:345–353.

Shaw, P.J., and E.G. Jordan. 1995. The nucleolus. *Annu. Rev. Cell Dev. Biol.* 11: 93–121.

Shepard, H.M., G.D. Lewis, J.C. Sarup, B.M. Fendly, D. Maneval, J. Mordenti, I. Figari, C.E. Kotts, M.A. Palladino, A. Ullrich, et al. 1991. Monoclonal antibody therapy of human cancer: taking the HER2 protooncogene to the clinic. *J. Clin. Immunol.* 11:117–127.

Srinivasan, R., C.E. Gillett, D.M. Barnes, and W.J. Gullick. 2000. Nuclear expression of the c-erbB-4/HER-4 growth factor receptor in invasive breast cancers. *Cancer Res.* 60:1483–1487.

Stachowiak, M.K., P.A. Maher, A. Joy, E. Mordechai, and E.K. Stachowiak. 1996. Nuclear accumulation of fibroblast growth factor receptors is regulated by multiple signals in adrenal medullary cells. *Mol. Biol. Cell.* 7:1299–1317.

Vecchi, M., S. Polo, V. Poupon, J.W. van-De-Loo, A. Benmerah, and P.P. Di-Fiore. 2001. Nucleocytoplasmic shuttling of endocytic proteins. *J. Cell Biol.* 153:1511–1518.

Waterman, H., I. Alroy, S. Strano, R. Seger, and Y. Yarden. 1999. The C-terminus of the kinase-defective neuregulin receptor ErbB-3 confers mitogenic superiority and dictates endocytic routing. *EMBO J.* 18:3348–3358.

Xie, Y., and M.C. Hung. 1994. Nuclear localization of p185neu tyrosine kinase and its association with transcriptional transactivation. *Biochem. Biophys. Res. Commun.* 203:1589–1598.